Eur. Phys. J. B 45, 213–218 (2005)
DOI: 10.1140/epjb/e2005-00124-5

THE EUROPEAN
PHYSICAL JOURNAL B

Structural analysis of ion irradiated polycrystalline NiFe/FeMn exchange bias systems

S. Blomeier[1,a], D. McGrouther[2], S. McVitie[2], J.N. Chapman[2], M.C. Weber[1], B. Hillebrands[1], and J. Fassbender[3]

[1] Fachbereich Physik and Forschungsschwerpunkt MINAS, Erwin-Schrödinger-Strasse 56, Technische Universität Kaiserslautern, 67663 Kaiserslautern, Germany
[2] Department of Physics and Astronomy, Kelvin Building, University of Glasgow, Glasgow G12 8QQ, Scotland, UK
[3] Institut für Ionenstrahlphysik und Materialforschung, Forschungszentrum Rossendorf, Postfach 510119, 01314 Dresden, Germany

Received 3 September 2004 / Received in final form 6 December 2004
Published online 19 April 2005 – © EDP Sciences, Società Italiana di Fisica, Springer-Verlag 2005

Abstract. Structural investigations of the ion irradiated polycrystalline NiFe/FeMn exchange bias bilayer system were carried out by means of transmission electron microscopy. Key structural parameters like average grain size, lattice constant, and texture, as well as their dependence upon ion irradiation were determined. This information was extracted from a detailed analysis of a series of bright field images, dark field images, and diffraction patterns. Furthermore a previously established model was tested which ascribes changes in the magnetic properties upon irradiation with 5 keV He^+ ions to the creation of point defects within the antiferromagnetic layer and to the intermixing between the ferromagnetic and antiferromagnetic layers. The obtained results indirectly support this model by excluding a change of the aforementioned structural parameters as a possible source of the observed modifications of the magnetic properties.

PACS. 61.80.Jh Ion radiation effects – 68.37.Lp Transmission electron microscopy (TEM) (including STEM, HRTEM, etc.) – 75.70.Cn Magnetic properties of interfaces (multilayers, superlattices, heterostructures)

1 Introduction

The investigation of ion irradiated thin magnetic films and multilayers is an area of great interest. It has been demonstrated that properties such as magnetic anisotropy (in CoPt multilayers or FePt alloys) [1–3] and the shift field of exchange biased bilayers, referred to as the exchange bias field [4], can be modified by means of ion irradiation [5–8]. As the respective irradiation techniques have a high spatial resolution and do not affect the surface topography of the bombarded samples, they promise a considerable potential for the fabrication of magnetic nanostructures. Therefore these techniques are of fundamental importance for the construction of magnetic data storage and sensor elements [9]. Within this context, it is of particular importance to discern the basic physical mechanisms underlying the observed irradiation-induced magnetic changes in the systems of interest. Although a model has been proposed that ascribes the modification of the shift field in exchange bias systems, consisting of a ferromagnetic (F) and an adjacent antiferromagnetic (AF) layer, to the creation of defects and intermixing between these layers [5], no experimental data concerning the structural nature of the origin of these modifications had been provided so far. For this reason, a series of experiments was conducted to investigate the structural properties of the polycrystalline $Ni_{81}Fe_{19}/Fe_{50}Mn_{50}$ exchange bias bilayer system, irradiated with either 5 keV He^+ or 30 keV Ga^+ ions. The dependence of key structural parameters such as lattice constant, texture, and average grain size on the applied ion dose was determined within a fluence regime of up to 1×10^{17} ions/cm^2 for He^+ and 5×10^{15} ions/cm^2 for Ga^+ ions, respectively. The results obtained from these experiments support the aforementioned model of irradiation-induced control of the exchange bias field indirectly by excluding a relation between these parameters and the observed modifications of magnetic properties of the investigated system.

2 Experiments

The system of interest consists of a $Ni_{81}Fe_{19}/Fe_{50}Mn_{50}$ (5 nm/10 nm) exchange bias bilayer which is covered by a 2 nm thick Cr cap layer to protect the sample from oxidation. All samples were prepared at room temperature using a molecular beam epitaxy system at a base pressure of 5×10^{-9} mbar. An electron-transparent Si_3N_4 membrane covered by a 15 nm thick Cu buffer layer was used

[a] e-mail: blomeier@physik.uni-kl.de

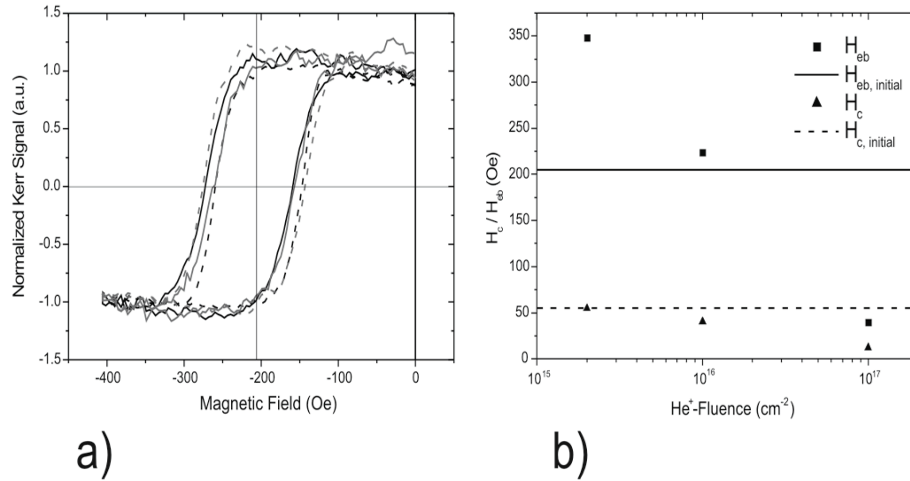

Fig. 1. (a) Normalized hysteresis loops measured by Kerr magnetometry from the four simultaneously grown samples before irradiation. All samples exhibit virtually identical magnetic properties, including a shift field of 205 ± 5 Oe and an easy axis coercivity of 55 ± 5 Oe. (b) Measured values of shift field H_{eb} and coercivity H_c for three of the samples after irradiation with fluences of 2×10^{15}, 1×10^{16}, and 1×10^{17} ions/cm^2 of 5 keV He$^+$ ions. The lines mark the initial values of H_{eb} (solid line) and H_c (dashed line) for comparison. At a fluence of 2×10^{15} ions/cm^2, the shift field is increased by about 75%. For the highest fluence, both shift field and coercivity are decreased below their initial values.

as a growth template, and exchange bias was initialized after deposition by means of a magnetic field cooling procedure. The latter involves the samples being heated up to 230 °C for 5 minutes and then cooled down below the blocking temperature $T_b = 155$ °C of the system in the presence of an external field of 500 Oe.

The irradiation with 5 keV He$^+$ ions was carried out with a modified VG Microtech EX05 ion source which is integrated into the UHV system used for the preparation process. Four samples, grown simultaneously to ensure the comparability of the obtained results, were irradiated with different fluences of 5 keV He$^+$ ions, ranging from 0 to 1×10^{17} ions/cm^2. Each sample was magnetically characterized by means of longitudinal Kerr magnetometry before and after irradiation. Before irradiation, all four samples exhibit virtually identical magnetic properties, as shown in Figure 1a. After irradiation, the respective values for both the easy axis coercivity H_c and the exchange bias field H_{eb} were found to be in accordance with the fluence dependence of these parameters derived from previous experiments [5,10]. Although the experiments described in [5] were carried out in an external field, it was found that it is not necessary to apply such a field during irradiation in order to modify H_{eb}. If one does not apply an external field, the dependence of H_{eb} on the applied ion fluence is identical to the case where the external field is parallel to the field applied during the procedure to initialize the exchange bias (see also, for example, [10]). This can be explained due to the fact that for our material system we have the situation that $H_{eb} \gg H_c$, thus the exchange bias field acts as an internal field which is sufficient to saturate the sample even when no external field is applied. The fluence dependence of H_{eb} and H_c derived from the Kerr measurements after irradiation is shown in Figure 1b. All Kerr measurements were carried out in easy axis geometry, using the second harmonic of a mode-locked Nd:YVO_4 laser (wave length $\lambda = 532$ nm, angle of incidence $\theta = 55°$) as a light source.

For the irradiation with 30 keV Ga$^+$ ions, an FEI Strata 200XP Focused Ion Beam system was used. In this case, a specific test pattern which consists of nine adjacent-lying rectangles, 10×400 μm^2 in dimension, was written onto an additional sample of the same composition. Each of these rectangles was irradiated with a different ion fluence ranging from 0 to 5×10^{15} ions/cm^2, using a beam current of 1000 pA. Thus it was possible to study the effects of the irradiation with different fluences of 30 keV Ga$^+$ ions on a single sample. The long axis of the aforementioned rectangles was chosen to be parallel to the bias field direction.

The structural analysis of the irradiated samples was carried out by means of transmission electron microscopy, using a JEOL 2000FX system. Bright field images, dark field images, and diffraction patterns were taken from the irradiated specimen (or regions, in the case of the irradiation with Ga$^+$ ions) which had been exposed to different ion fluences. Typical examples of such images are shown in Figure 2. Both bright field (Fig. 2a) and dark field images (Fig. 2b) were then analyzed to determine grain sizes within the multilayer stack, while the diffraction patterns (Fig. 2c) allowed us to discern the crystallographic structure of the material system. In particular, lattice type, degree of texture, and an averaged value for the lattice constant could be extracted in this way. For the analysis of the bright field images the software package "Height-Height-Correlation v.1.10" [11] was used, which determines the correlation length l from a given grayscale image. This parameter describes the length scale of correlated features and was taken as a rough measure of the average grain size within the images. Mean particle sizes

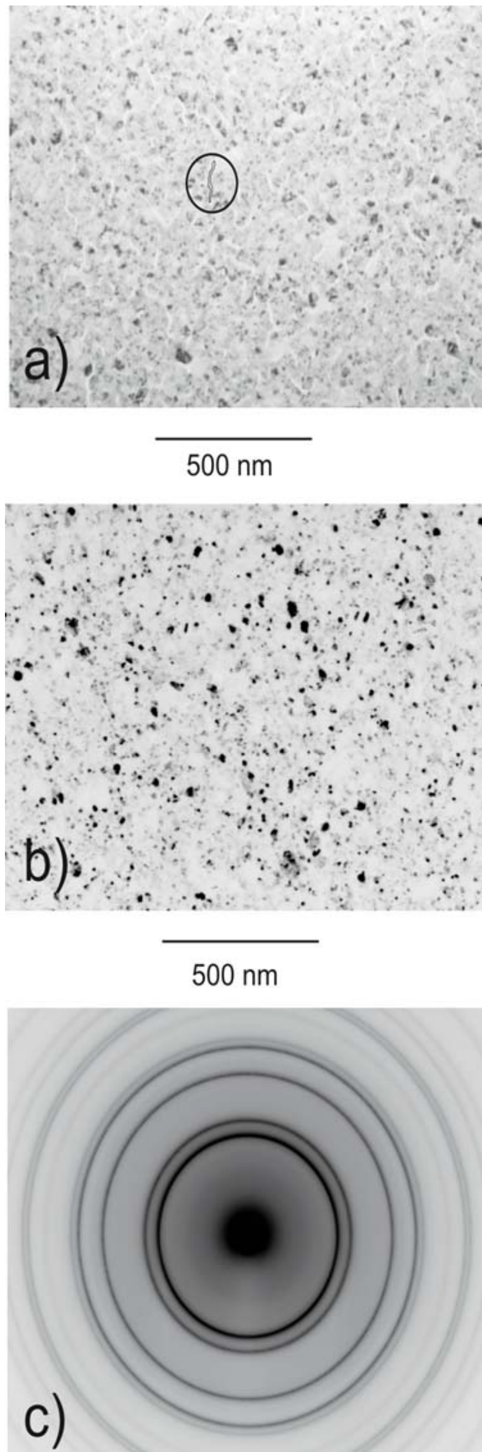

Fig. 2. (a) Typical bright field image taken from a non-irradiated sample by means of transmission electron microscopy. The granular microstructure of the investigated sample is clearly visible. One of the cracks observable in the image is encircled and highlighted. (b) Typical TEM dark field image. The image shows the same sample and area as in panel (a). A section of the (111) and (200) diffraction rings was selected to form the image. The image displayed here is a negative. Individual grains become clearly visible in this imaging mode. (c) Typical diffraction pattern taken from a non-irradiated sample.

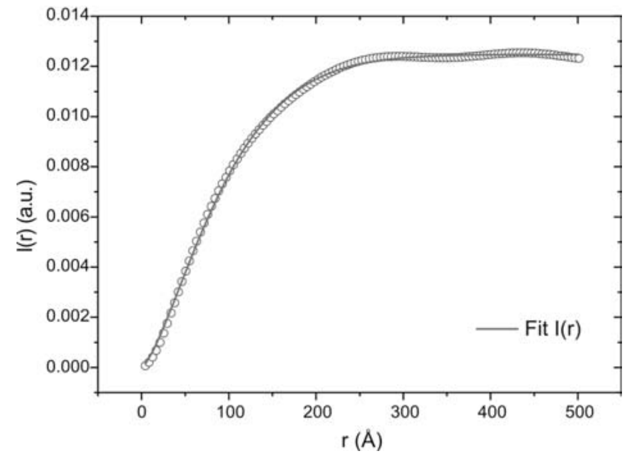

Fig. 3. Intensity correlation of a typical bright field image. The solid line is a fit according to equation (1), which in this case yields a value of $l = 10.3 \pm 0.1$ nm for the correlation length. The fit model used can reproduce the experimental data very well.

were also determined from dark field images by direct measurements of a large number of individual grains. In order to investigate the degree of texture within the investigated system, diffraction patterns were taken from the samples after tilting them within the electron optical column of the transmission electron microscope.

3 Results

First, the obtained bright field images were analyzed. Within these images, the granular microstructure of the investigated samples is clearly visible. Multiple structural "cracks" on the nanometer scale were observed in every image (see Fig. 2a). Studies of a test sample which consisted only of the copper buffer allowed us to locate these cracks in that part of the multilayer stack. They contribute to a deterioration of the magnetic contrast in Fresnel images taken from the investigated samples during another series of experiments described elsewhere [8]. The cracks indicate that copper exhibits a very irregular growth behavior on top of the Si_3N_4 membrane substrates that were used for the preparation process under the growth conditions mentioned in Section 2.

Figure 3 shows a typical result derived from the analysis of a bright field image that was taken from a non-irradiated sample. The data displayed represents the intensity correlation as a function of the lateral distance within the given grayscale image. The solid line is a fit according to the model

$$I(r) = 2\omega^2(1 - \exp(-(r/l)^{2\alpha})), \quad (1)$$

where r is the lateral distance and $I(r)$ describes the intensity correlation as a function of r. Equation (1) is a standard model which is normally used for the analysis of STM images [12] and which includes three parameters, denoted by ω (RMS roughness), α (roughness exponent), and l (correlation length). However, since the image investigated here is a TEM image, which contains information

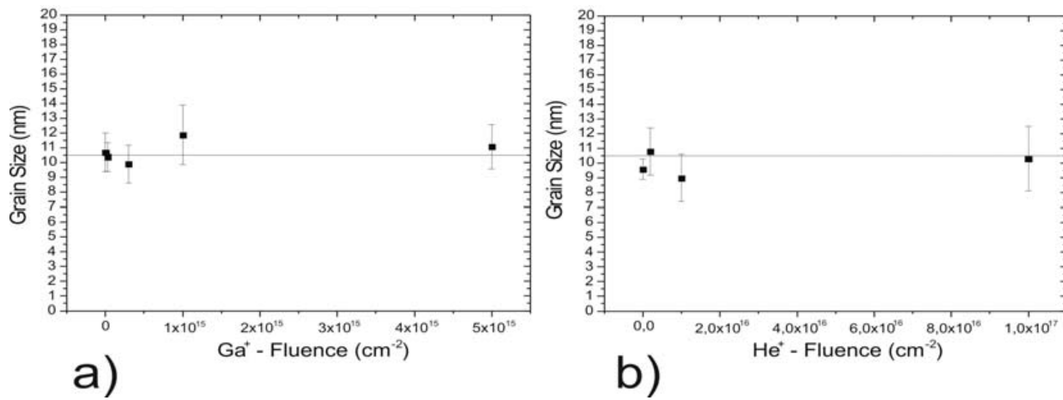

Fig. 4. Average particle sizes from irradiated specimen as a function of the fluence applied during the irradiation with a) 30 keV Ga^+ ions and b) 5 keV He^+ ions. An average value of $l = 10.5$ nm is found (marked by a line in each graph), which does not change significantly with increasing ion fluence in both cases.

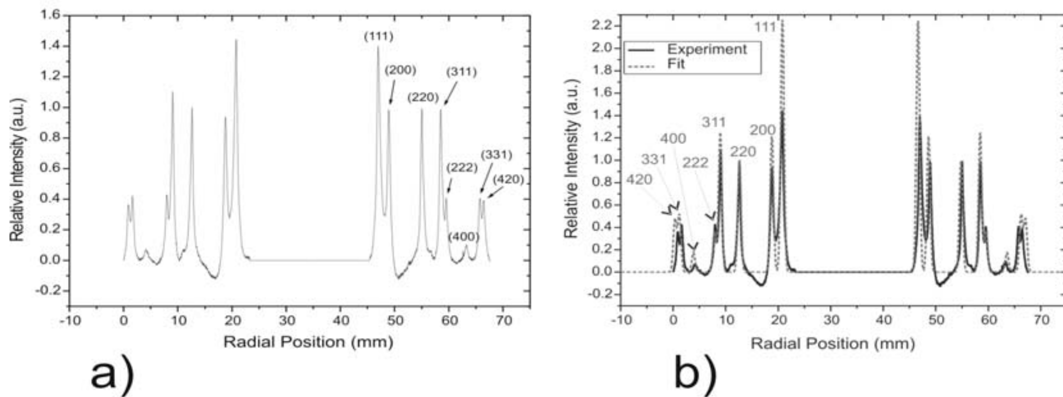

Fig. 5. (a) Line profile taken from a diffraction pattern as shown in Figure 2c. Background intensity has been reduced from the image, and the central peak has been removed. The pattern displayed shows an fcc-structure with a lattice constant of $a = 3.57 \pm 0.03$ Å. The Miller indices of each diffraction ring are indicated in the right half of the diagram. (b) Fit of the line profile using a lattice constant of $a = 3.57 \pm 0.03$ Å. The fit is normalized to the height and the radial position of the left (220) peak. The width of the peaks has been fitted (assuming Gaussian profiles), while their relative intensities have been calculated, using a relativistic Mott scattering cross-section [22]. The intensities of the innermost experimental peaks are significantly lower than their theoretical counterparts because the film which was used to record the diffraction pattern is already saturated in this area.

from a multilayer stack and not from a surface with a given roughness, both ω and α do not contain information on the roughness of our samples. These parameters are a measure of the variation of grayscale values within a given image, which in this case is inherently related to the variation of the crystallographic orientation of the grains within the multilayer stack. However, this information is not relevant for our studies, as we pursue an alternative, much more convenient approach to determine the texture of the investigated samples, by tilting the specimen within the electron optical column of the JEOL 2000FX. On the other hand, l still describes the length scale of correlated features within the image and is taken as a rough measure for the average grain size within the investigated system.

This method of analysis was applied to a series of images that were taken from specimens which were exposed to different fluences of 5 keV He^+ or 30 keV Ga^+ ions. The results of this analysis are depicted in Figure 4. An average particle size of $l = 10.5 \pm 2$ nm is found, which does not significantly change with increasing ion fluence for both types of irradiation. The obtained value of about 10 nm for the average grain size is in good accordance with results from investigations of other polycrystalline exchange bias systems.

In order to check these results for consistency, individual grain sizes were also measured directly from the dark field images, using a commercial graphics package. An average value of about 9 nm for the mean particle size was found in this way, which is in good agreement with the value of 10.5 ± 2 nm obtained through the analysis of the bright field images. Furthermore dark field image analysis also confirmed no change in average grain size with dose.

Figure 5a shows a line profile of a typical diffraction pattern for a reduced background intensity. A fit to this profile, displayed by Figure 5b, yields an fcc-structure with a lattice constant of $a = 3.57 \pm 0.03$ Å. This measured lattice constant is in good accordance with the lattice constant values for the bulk materials of the elements (or alloys, respectively) present in the multilayer stack ($a_{\mathrm{Cu}} = 3.61$ Å, $a_{\mathrm{FeMn}} = 3.62$ Å, $a_{\mathrm{NiFe}} = 3.54$ Å). As

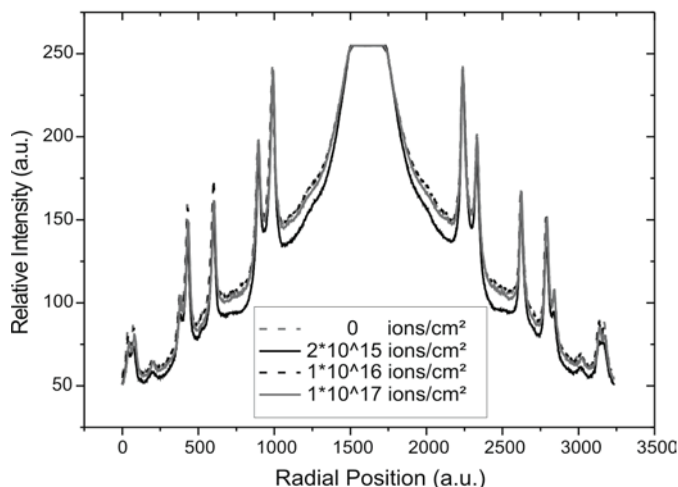

Fig. 6. Line profiles taken from the four simultaneously grown samples which were irradiated with different fluences of 5 keV He^+ ions as indicated in the inset.

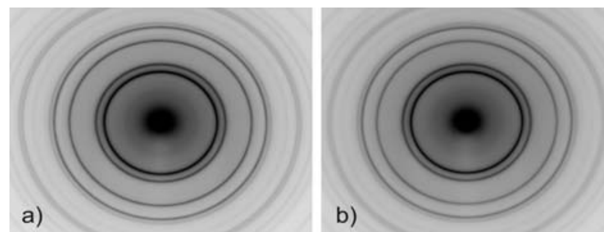

Fig. 7. Diffraction patterns taken from a sample under an angle of a) 90° or b) 52.5° to the direction of the electron beam. The patterns are identical within experimental error.

each layer has slightly different structural properties, this value is in fact an average taken from a narrow distribution of lattice constant values. This is indicated by a broadening of the peaks, as well as by a slight deviation of the radial position of some peaks from their theoretically predicted location. As can be seen from Figure 5b, the innermost experimental peaks are shifted slightly outward from their predicted position, while the outermost experimental peaks are closer to the center of the pattern than their theoretical counterparts. However, this method is not accurate enough to provide any reliable quantitative information about stress-induced effects on the lattice.

Line profiles obtained from diffraction patterns taken from specimens which were irradiated with different fluences of 5 keV He^+ ions are shown in Figure 6. A similar result is obtained for the irradiation with Ga^+ ions (not shown here). It is evident that the crystallographic and crystalline structure of the analyzed multilayer system do not change with increasing ion fluence.

Moreover, our investigations yield that there is no texture present in the system, i.e., it is a 3D randomly oriented polycrystalline system, as the obtained diffraction patterns do not change with variation of direction of the incident electron beam on the sample. As an example, Figure 7 compares a diffraction pattern taken from a non-irradiated sample under an angle of 52.5° to the direction of the electron beam to the standard pattern which is taken under an angle of 90°. A detailed line profile analysis yields that both patterns are identical within experimental error. Furthermore, it was found that the irradiation process does not induce any texture within the investigated system.

4 Discussion and outlook

The work presented here suggests that transmission electron microscopy is a powerful tool to determine the structural properties of magnetic materials. Additional studies (not shown here) were conducted to investigate the magnetic properties of the studied exchange bias system upon irradiation with 5 keV He^+ and 30 keV Ga^+ ions by means of the Fresnel mode of Lorentz microscopy [8].

For the chemically disordered, untextured NiFe/FeMn system investigated here, the results presented above indicate that neither granular growth nor structural ordering processes take place upon ion irradiation. Moreover, the observed independence of the average grain size on the applied ion fluence suggests that the previously observed magnetic modifications within the system of interest correspond to structural changes of a different nature. Studies of Poppe et al. [6] have shown that at least two separate mechanisms are responsible for the modification of the exchange bias effect upon irradiation with 5 keV He^+ ions. One of these mechanisms was found to be an interfacial effect and is believed to be a result of interfacial intermixing, while the other effect was demonstrated to originate from the bulk of the irradiated samples. Stopping and Range of Ions in matter (SRIM) simulations concerning the irradiation of our material system with either 5 keV He^+ or 30 keV Ga^+ ions indicate that interfacial intermixing processes, i.e., the dislocation of Ni atoms into the antiferromagnet and the disclocation of Mn atoms into the ferromagnet, are indeed triggered by the ion bombardment [13,14].

It is known that interfacial intermixing in multilayer systems can lead to the formation of alloys, which consist of the elements of two originally adjacent, but separate layers. Investigations by Spenato et al. [15] and by Ben Youssef et al. [16] revealed that such a formation takes place for sputtered NiFe/Mn and NiFe/NiMn bilayers, which are composed of the same elements as the NiFe/FeMn system studied here. However, in their case the interfacial intermixing was found to occur upon annealing of the respective systems, not upon irradiation with keV ions.

The formation of an interfacial alloy results in a nonmagnetic spacer layer which separates the layers that contributed to its creation process. Experiments performed by Gökemeijer et al. [17] and by Mewes et al. [18] yielded that such an interfacial spacer leads to an exponential decrease of the exchange bias field, which is indeed observed for the irradiation with 30 keV Ga^+ ions [8] and for the irradiation with high fluences of He^+ ions [5].

The experimental situation concerning the bulk contribution, which leads to an enhancement of the exchange bias field, is less clear. A model proposed by Mougin et al. [5] attributes this enhancement, observed

in the case of irradiation with fluences of the order of 2×10^{15} ions/cm^2 of 5 keV He$^+$ ions, to the creation of point defects within the antiferromagnetic layer, which act as pinning sites for the formation of domain walls (on such pinning sites, see also [19–21]). No direct experimental proof that such point defects are created and are indeed correlated to the enhancement of the shift field has been reported in the literature. However, with the work presented here we can exclude several alternative mechanisms which might be the origin of the obtained magnetic modifications. In particular, we have demonstrated that neither grain growth nor a large-scale change in the crystallographic structure of our system can be responsible for the observed irradiation-induced effects. Thus, our work indirectly supports the aforementioned model.

Possible future experiments in this direction might include a HRTEM analysis of cross-sectional specimens which are taken from the interface region between ferromagnetic and antiferromagnetic layer, in combination with element-sensitive nanoanalytical methods. Within this context it is of particular interest to determine whether a relationship between intermixing effects and the magnetic properties of the investigated samples can indeed be proven experimentally.

In summary, a detailed structural analysis of the ion-irradiated NiFe/FeMn exchange bias system by means of transmission electron microscopy has shown that key structural parameters like average grain size, lattice constant, and texture remain unchanged upon ion irradiation. By excluding a change of these parameters as a possible source for the observed irradiation-induced modifications of the exchange bias field, these results indirectly support a previously established model, which ascribes the observed magnetic modifications of the investigated system to the creation of point defects and intermixing of the ferromagnetic and antiferromagnetic layer.

This work is supported in part by the Deutsche Forschungsgemeinschaft and the European Communities Human Potential program under Contract No. HPRN-CT-2002-00296 NEXBIAS. One of the authors (M.C.W.) would like to acknowledge support by the Graduiertenkolleg 792 “Nichtlineare Optik und Ultrakurzzeitphysik” of the Deutsche Forschungsgemeinschaft.

References

1. C. Chappert, H. Bernas, J. Ferre, V. Kottler, J.P. Jamet, Y. Chen, E. Cambril, T. Devolder, F. Rousseaux, V. Mathet, H. Launois, Science **280**, 1919 (1998)
2. T. Devolder, C. Chappert, Y. Chen, E. Cambril, H. Bernas, J.P. Jamet, J. Ferré, Appl. Phys. Lett. **74**, 3383 (1999)
3. D. Ravelosona, C. Chappert, V. Mathet, H. Bernas, Appl. Phys. Lett. **76**, 236 (2000)
4. A.P. Malozemoff, Phys. Rev. B **35**, 3679 (1987)
5. A. Mougin, T. Mewes, M. Jung, D. Engel, A. Ehresmann, H. Schmoranzer, J. Fassbender, B. Hillebrands, Phys. Rev. B **63**, R060409 (2001)
6. S. Poppe, J. Fassbender, B. Hillebrands, Europhys. Lett. **66**, 430 (2004)
7. D. McGrouther, J.N. Chapman, F.W.M. Vanhelmont, J. Appl. Phys. **95**, 7772 (2004)
8. S. Blomeier, D. McGrouther, R. O'Neill, S. McVitie, J.N. Chapman, M.C. Weber, B. Hillebrands, J. Fassbender, J. Magn. Magn. Mater., `10.1016/j.jmmm.2004.11.278`
9. J. Fassbender, S. Poppe, T. Mewes, J. Juraszek, B. Hillebrands, K.-U. Barholz, R. Mattheis, D. Engel, M. Jung, H. Schmoranzer, A. Ehresmann, Appl. Phys. A **77**, 51 (2003)
10. A. Mougin, T. Mewes, R. Lopusnik, M. Jung, D. Engel, A. Ehresmann, H. Schmoranzer, J. Fassbender, B. Hillebrands, IEEE Trans. Magn. **36**, 2647 (2000)
11. T. Mewes, *Height-Height-Correlation v. 1.10 – Software zur Bestimmung der Höhenkorrelationsfunktion aus Rastersonden-Mikroskopie-Daten, Universität Kaiserslautern*
12. H.N. Yang, Y.P. Zhao, A. Chan, T.M. Lu, G.C. Wang, Phys. Rev. B **56**, 4224 (1997)
13. J.F. Ziegler, J.F. Biersack, J.P. Littmark: *The Stopping and Range of Ions in Solids*. Pergamon, New York (1985)
14. J.F. Ziegler, *Documentation of the SRIM code*, `www.srim.org` (2003)
15. D. Spenato, J. Ben Youssef, H. Le Gall, J. Appl. Phys. **89**, 6898 (2001)
16. J. Ben Youssef, D. Spenato, H. Le Gall, Magnetics Conference, 2002. INTERMAG Europe 2002. Digest of Technical Papers. 2000 IEEE International
17. N.J. Gökemeijer, T. Ambrose, C.L. Chien, Phys. Rev. Lett. **79**, 4270 (1997)
18. T. Mewes, B.F.P. Roos, S.O. Demokritov, B. Hillebrands, J. Appl. Phys. **87**, 5064 (2000)
19. P. Miltèny, M. Gierlings, J. Keller, B. Beschoten, G. Güntherodt, Phys. Rev. Lett. **84**, 4224 (2000)
20. U. Nowak, K.D. Usadel, J. Keller, P. Miltény, B. Beschoten, G. Güntherodt, Phys. Rev. B **66**, 014430 (2002)
21. J. Keller, P. Miltény, B. Beschoten, G. Güntherodt, U. Nowak, K.D. Usadel, Phys. Rev. B **66**, 014431 (2002)
22. L. Reimer, *Scanning Electron Microscopy. Physics of Image Formation and Microanalysis*, 2nd edn. (Springer Verlag, Berlin, Heidelberg, New York, 1998)